NASA/TM–20240001596

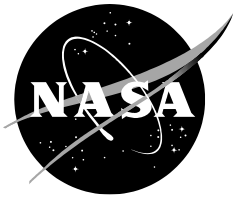

The Effects of Impactor Shape on the Compression After Impact Strength of Carbon/Epoxy Face Sheet Aluminum Honeycomb Core Sandwich Structure

Alan T. Nettles
Willian E. Guin
Baxter W. Barnes
James P. Mavo
Marshall Space Flight Center, Huntsville, Alabama

February 2024

NASA STI Program Report Series

The NASA STI Program collects, organizes, provides for archiving, and disseminates NASA's STI. The NASA STI program provides access to the NTRS Registered and its public interface, the NASA Technical Reports Server, thus providing one of the largest collections of aeronautical and space science STI in the world. Results are published in both non-NASA channels and by NASA in the NASA STI Report Series, which includes the following report types:

- TECHNICAL PUBLICATION. Reports of completed research or a major significant phase of research that present the results of NASA Programs and include extensive data or theoretical analysis. Includes compilations of significant scientific and technical data and information deemed to be of continuing reference value. NASA counterpart of peer-reviewed formal professional papers but has less stringent limitations on manuscript length and extent of graphic presentations.

- TECHNICAL MEMORANDUM. Scientific and technical findings that are preliminary or of specialized interest, e.g., quick release reports, working papers, and bibliographies that contain minimal annotation. Does not contain extensive analysis.

- CONTRACTOR REPORT. Scientific and technical findings by NASA-sponsored contractors and grantees.

- CONFERENCE PUBLICATION. Collected papers from scientific and technical conferences, symposia, seminars, or other meetings sponsored or co-sponsored by NASA.

- SPECIAL PUBLICATION. Scientific, technical, or historical information from NASA programs, projects, and missions, often concerned with subjects having substantial public interest.

- TECHNICAL TRANSLATION. English-language translations of foreign scientific and technical material pertinent to NASA's mission.

Specialized services also include organizing and publishing research results, distributing specialized research announcements and feeds, providing information desk and personal search support, and enabling data exchange services.

For more information about the NASA STI program, see the following:

- Access the NASA STI program home page at http://www.sti.nasa.gov

- Help desk contact information:

https://www.sti.nasa.gov/sti-contact-form/ and select the "General" help request type.

NASA/TM–20240001596

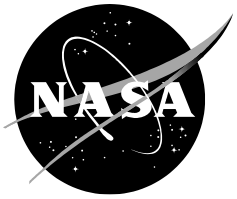

The Effects of Impactor Shape on the Compression After Impact Strength of Carbon/Epoxy Face Sheet Aluminum Honeycomb Core Sandwich Structure

Alan T. Nettles
Willian E. Guin
Baxter W. Barnes
James P. Mavo
Marshall Space Flight Center, Huntsville, Alabama

National Aeronautics and
Space Administration

Marshall Space Flight Center
Huntsville, Alabama 35812

February 2024

1. INTRODUCTION

For damage tolerance testing of polymer matrix composites, impact damage is typically inflicted using a rounded tip impactor to represent a generic impact event. The ASTM standard for Compression After Impact (CAI) testing [1] calls for a blunt, hemispherical striker tip, although it does state that the use of a sharp striker tip may be appropriate in certain circumstances. In actual practice, many different forms of impactor shapes can impact a composite structure; from very large impactors such as bumpers on ground handling equipment [2] to very small "puncture-type" impacts such as a Kevlar rocket motor case than was hit against a wall with a protruding stove bolt in 1991. This study will focus on the damage tolerance differences between two commonly used sized hemispherical impactors (12.7 mm and 24.5 mm) and a sharp tipped impactor.

Past studies that the authors are familiar with where sharp tip impactors were used involved damage tolerance of rocket motor cases [3-5]. For rocket motor cases, the laminate was shown to be so thick that there was little difference in the impact response of sharp versus blunt impactors. The thick laminate enabled the first few layers to crush at the tip of the sharp impactors and the debris of these first few plies acted as a "blunting mechanism" ahead of the sharp tip.

However, there is space flight hardware made of thinner laminates than those of rocket motor cases and some of these involve sandwich structure with relatively thin face sheets.

For thinner laminates some results in the open literature relevant to this current study were found comparing the impact response of different shape and size impactors [6-13]. Three of these references [6,10,13] provided post impact compression strength results and two utilized sandwich structure [6,13]. The results showed that, as far as the impact response, of commonality in all these studies was that, for a given impact energy, the damage size as determined by non-destructive evaluation (NDE) techniques was smaller for the sharper (or smaller diameter) impactors and dent depth was larger for the sharper or smaller diameter impactors. For CAI strength response, mixed results were found. One study that utilized sandwich structure [6] showed that, in general, the larger impactor gave lower CAI values for a given impact energy but another study [10] showed that a larger diameter impactor gave higher CAI strength values for a given impact energy. A study using foam core sandwich structure [13] found mixed results in that the CAI strength was lower for a sharp tipped impactor at low impact energy values, but higher at higher impact energy levels.

This study examined the effect of impactor shape (sharp tip) and diameter (12.7 and 25.4 mm) on the CAI strength response of aluminum honeycomb core sandwich structure that may be used for launch vehicle structure.

2. MATERIALS

The face sheets of the sandwich specimens tested in this study consisted of IM7 carbon fiber with 8552-1 epoxy resin and were co-cured to the aluminum honeycomb core which had a density of 72 kg/m^3, cell size of 3.175 mm and 2.54 cm thickness. All the face sheets were manufactured by automated fiber placement (AFP) at NASA's MSFC. The layup for the face sheets was 8-ply $[-45/90/+45/0]_S$ quasi-isotropic with the 0º fiber direction coinciding with the "L" direction of the honeycomb. The sandwich structure had a layer of FM 300-2M epoxy film adhesive placed over the core prior to the automated tape laying process used to manufacture the face sheets.

The sandwich structure was cured in an autoclave with a pressure of 276 kPa and a temperature of 175 ºC. The flat sandwich panel made for this study was 122 cm × 61 cm in size. The sandwich structure showed good consolidation with some minor porosity in the bottom plies as seen in the cross-sectional photomicrographs shown in figure 1. Using photomicroscopy and measuring tools contained within the software attached to the microscope, the nominal face sheet thickness of the sandwich structure was measured at 1.27 mm.

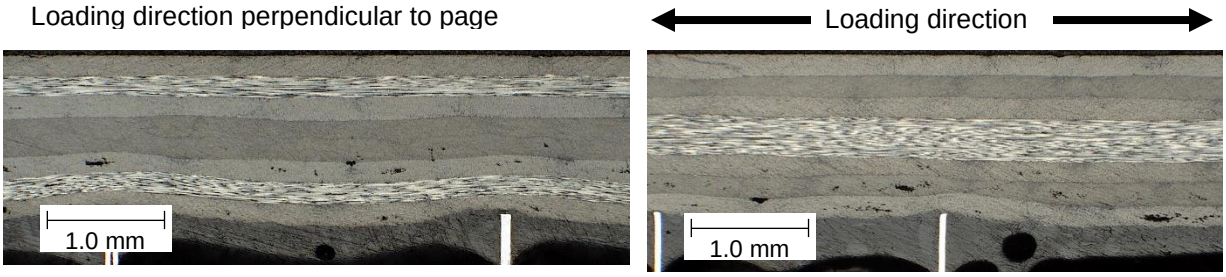

Figure 1. Cross sectional photomicrographs of a face sheet showing good consolidation and minor porosity in lower plies. Specimen cuts are in width direction (left) and loading direction (right).

The sandwich structure was cut into 15.2 cm tall (direction of loading) by 10.2 cm wide specimens using a diamond saw. The top and bottom edges of these specimens had to be filled with a paste epoxy to prevent end brooming. This was accomplished by crushing the core at the ends by about 6 mm as shown in figure 2a and then filling the channel with EA 9394 paste epoxy as shown in figure 2b.

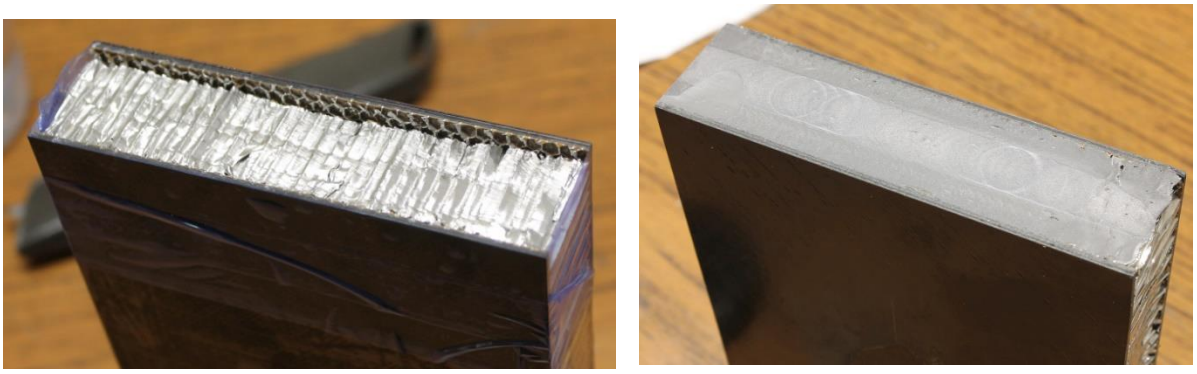

Figure 2. Photograph of the process to "pot" the ends to prevent end brooming during compression testing. **a)** crush the core down about 6 mm on ends and **b)** fill the resulting channel with epoxy paste adhesive.

The "potted" ends were then machined to ±0.0025 mm tolerance of parallelism using a vertical end mill with a solid carbide cutting tool (Onsrud 67-526 designed for carbon fiber machining). The side edges of the specimens were machined to be perpendicular to the top and bottom edges.

Undamaged strength testing of the sandwich structure was not pursued in this study since the undamaged specimens exhibited end-brooming despite the potted ends. This was deemed suitable since this study concerns damage tolerance testing and the differences between impactor shapes and sizes and the undamaged strength values are not relevant to the scope of this study.

3.0 IMPACT DAMAGE TESTING

An instrumented drop weight impact apparatus was used in this study. The mass and height of the impactor could be varied to get a variety of impact energies. A pneumatic rebound brake prevented multiple impacts on the specimen. Each specimen was clamped between two steel plates during impact. The top steel plate had an opening to allow the impactor to pass through and hit the specimen. The bottom plate was solid with no cutout.

Three impactors were used in this study, two hemispherical impactors, one of diameter 25.4 mm and one of 12.7 mm and a conical sharp tipped impactor with a diameter of 19.0 mm. Photographs of the three types of impactors are shown in figure 3.

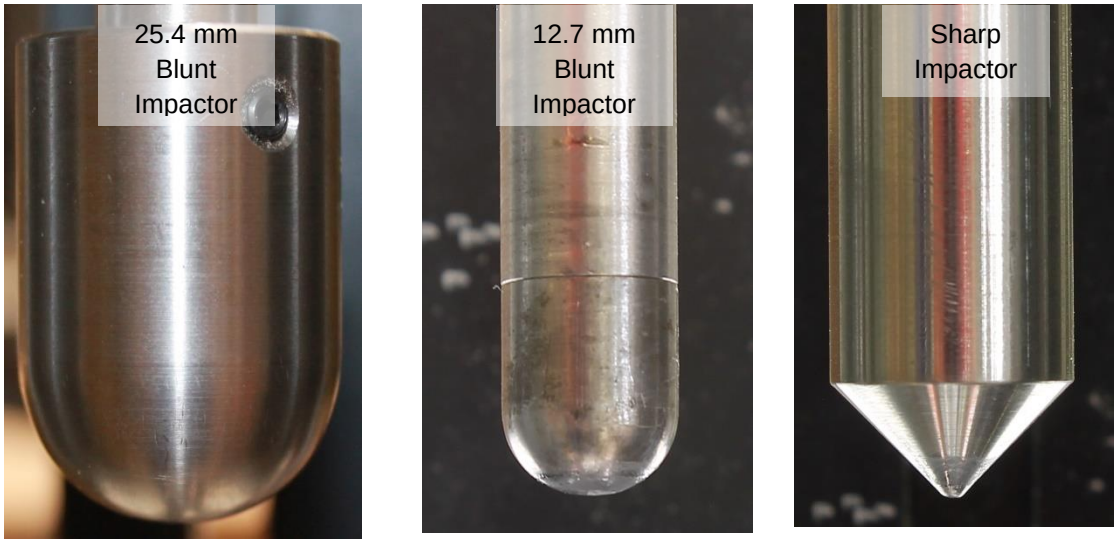

Figure 3. Photograph of three types of impactors used in this study.

Preliminary CAI strength testing showed that at impact energies less than 2.7 J failure was by end brooming and thus 2.7 J was chosen as a lower impact energy bound. At 8.1 J the 12.7 mm tup began to penetrate the face sheet, and this was chosen as an upper bound impact energy.

It was decided to test the specimens with all three types of impactors with these two impact energies bracketing the high and low impact energies and using one intermediate impact energy (5.4 J). Thus, the honeycomb core sandwich specimens were to be impacted at 2.7, 5.4 and 8.1 J with each of the three types of impactors for a total of nine impact conditions. Multiple specimens were tested at each of the nine impact conditions. Although the impacts were instrumented, the instrumented impact results (load-deflection curves) will not be presented here for two reasons. First, the load-deflection data was suspect for the sharp tip and 25.4 mm impactors since they were drastically different than static indentation results (excess “ringing” in the impact data was present despite applying numerous filters to the data). Second, in actual practice an object that may impact a composite part is not instrumented and thus the instrumented data is only of academic interest and does little to help disposition an actual impact event. Thus, only post impact parameters (ones that could be measured in the field) were measured and assessed in this study.

3.1 Visual Damage

Examples of the visual damage caused by each of the nine impact conditions are shown in the photographs in figure 4. The main takeaway from the visual impact results is that the damage from the sharp impactor is easier to see and will result in a lower impact energy for any visual damage threshold than the blunt impactors. This is not an unexpected result. The difference in visual damage between the 12.7 mm and 25.4 mm impactors is not as notable except at the highest impact energy used which is when penetration of the 12.7 mm impactor began.

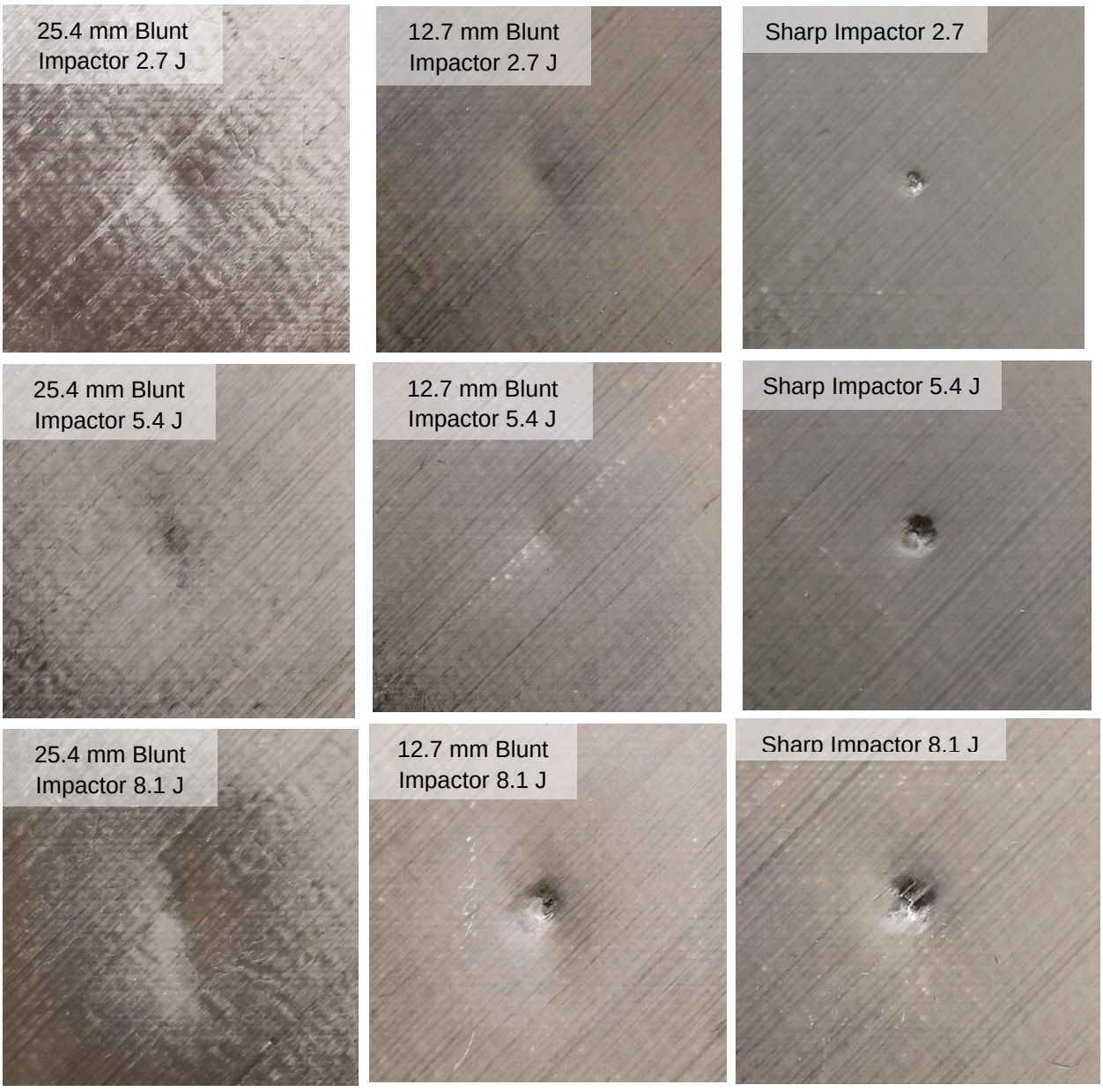

Figure 4. Examples of visual damage inflicted upon the specimens at each of the nine impact conditions tested. Loading direction is from top to bottom in these pictures.

3.2 Dent Depth Results

For each impacted specimen, the depth of the dent caused by the impact was measured at least 24 hours after the impact to allow for any “dent relaxation”. A dial gage was used to measure the dent depths and is shown in figure 5.

Figure 5. Dial gage used in this study to measure dent depths of impacted specimens.

The results of dent depth versus impact energy are plotted in figure 6.

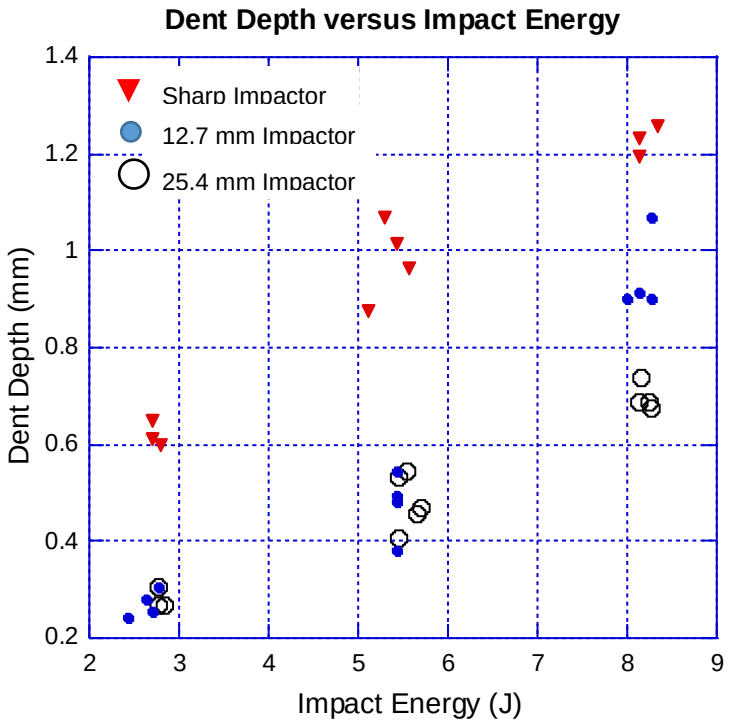

Figure 6. Dent depth versus impact energy for the specimens tested in this study.

The results in figure 6 show that, for all impact energies used, the sharp tipped impactor gave deeper dent depths. There was little difference between the dent depths of the two hemispherical impactors except at the highest impact energy where the larger impactor gave a smaller dent depth.

3.3 Thermography Results

Non-destructive evaluation (NDE) in the form of thermography was performed on the impacted specimens and sample signatures from each of the nine impact conditions are presented in figure 7. The shape of the damage zone is basically circular for all three energy levels using the three impactors.

Since it has been claimed that damage width as detected by thermography is a good indicator of CAI strength [14], the width of the damage zones in figure 7 were measured. What constitutes the “damage width” is noted in the first thermography example in figure 7.

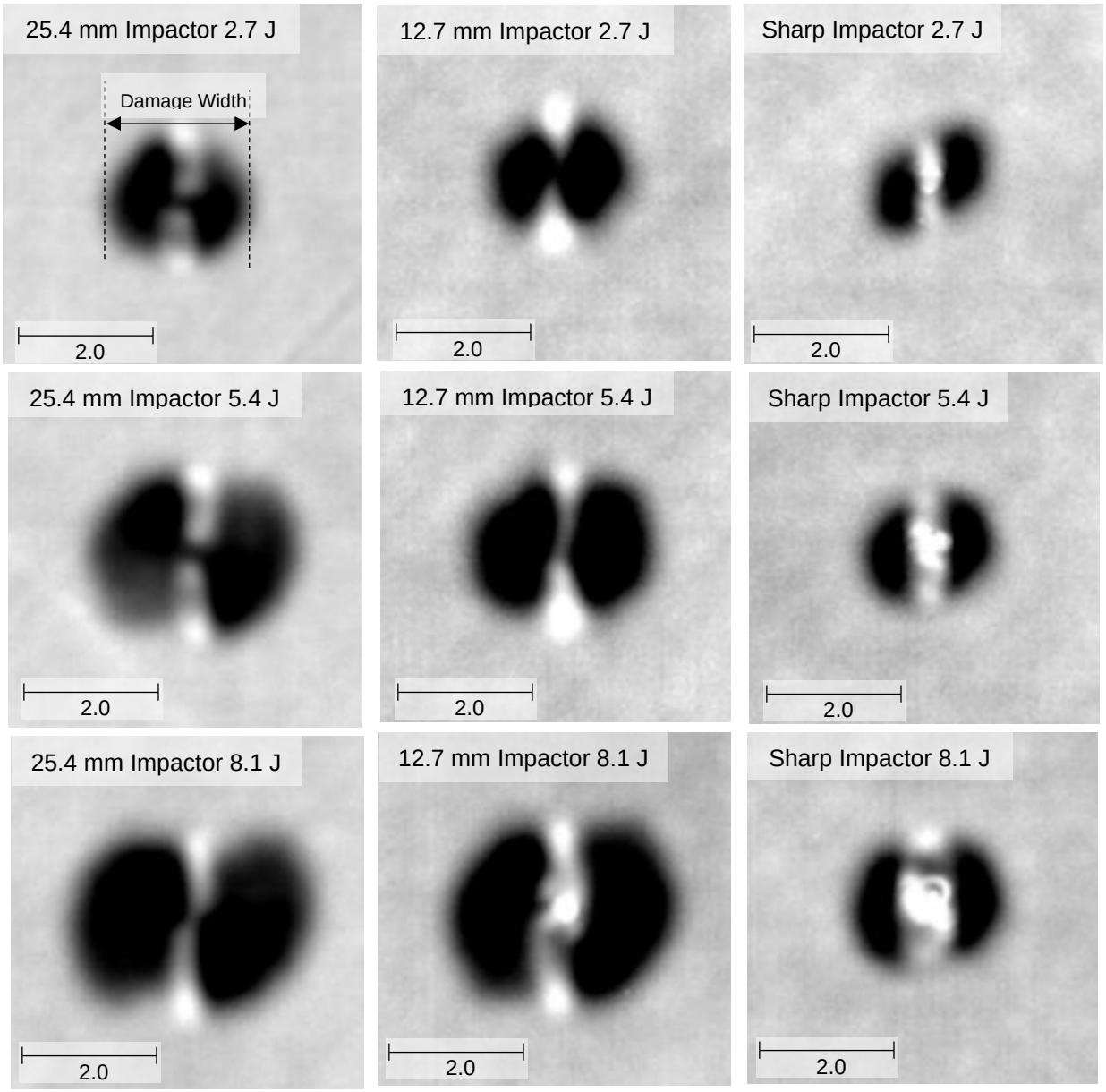

Figure 7. Examples of thermography images of the specimens at each of the nine impact conditions tested. Loading direction is from top to bottom in these pictures.

Damage size (width) as a function of impact energy is plotted in figure 8. A few of the impacted specimens did not have their damage width measured since the thermography apparatus was unavailable for a span of time and the residual strength data was needed to guide further testing.

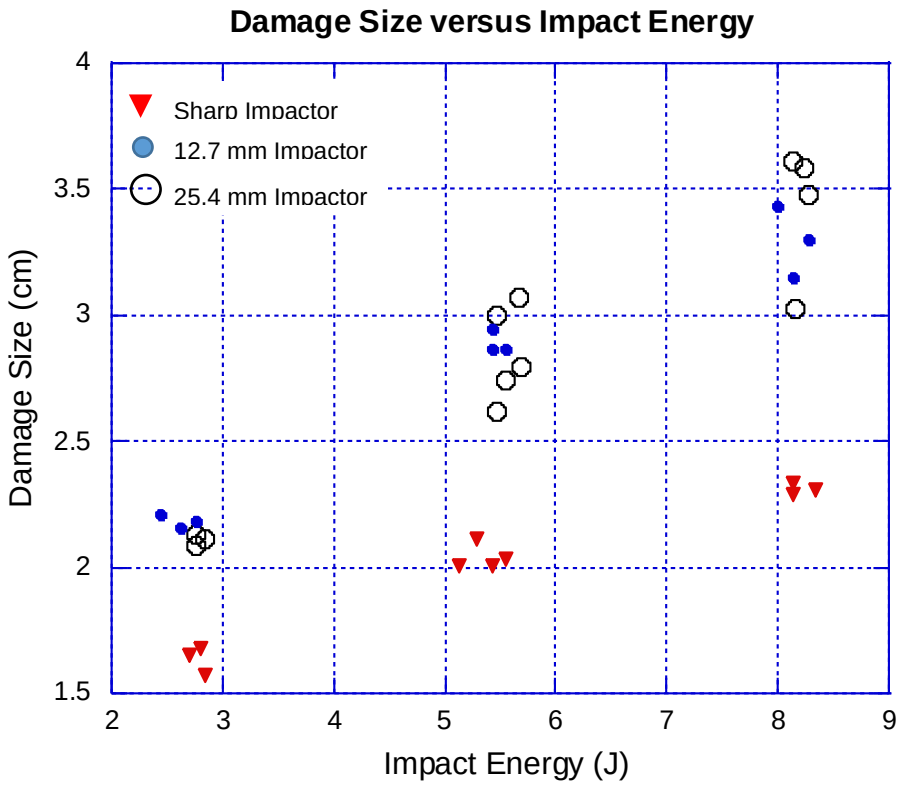

Figure 8. Damage size (width) versus impact energy for the specimens tested in this study.

The damage width is smaller at any given impact energy for the sharp tipped impactor indicating, that if the conclusion in [14] that damage width is a good predictor of CAI strength is correct then the sharp tipped impactors should give a higher CAI strength than the hemispherical impactors at any given impact energy. There is little difference in the damage size between the two hemispherical impactors.

4.0 COMPRESSION AFTER IMPACT TESTING

The impacted sandwich specimens were assessed for residual compression strength using the test fixture shown in figure 9. Three strain gages were placed on the specimen to ensure even loading of each of the face sheets. Two gages on the impact side were to ensure even loading across the specimen width and one gage in the center on the opposite (non-impacted) side to monitor for even loading across the specimen thickness. The specimens were taken to approximately 1000 microstrain compression and if one gage was lower than the others by more than 10%, shims were placed under the edge that was reading low until the gages were even. During compression testing the gages were monitored and if any deviation greater than 10% occurred, the test was stopped, and shims would be rearranged until the gages read within 10% of each other all the way until failure of the specimen.

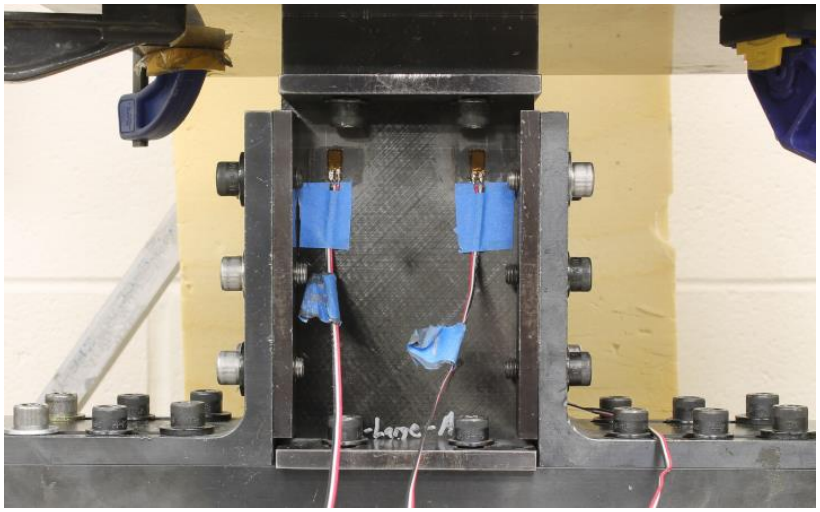

Figure 9. Fixture used in this study to assess compression after impact strength of sandwich specimens.

The CAI strength results are plotted versus impact energy in figure 10. Note that not all of the impacted specimens were tested for CAI strength as some were held for destructive microscopy testing and are thus not included in any of the following residual strength plots. Since a power curve fit has been shown to fit CAI versus damage severity well [14] a power curve fit has been applied across all the data (all three impactor types). Ideally a method of plotting all the CAI data that fits a power curve well is desired so that a CAI design allowable of reasonable fidelity for any shape or diameter impactor can be calculated.

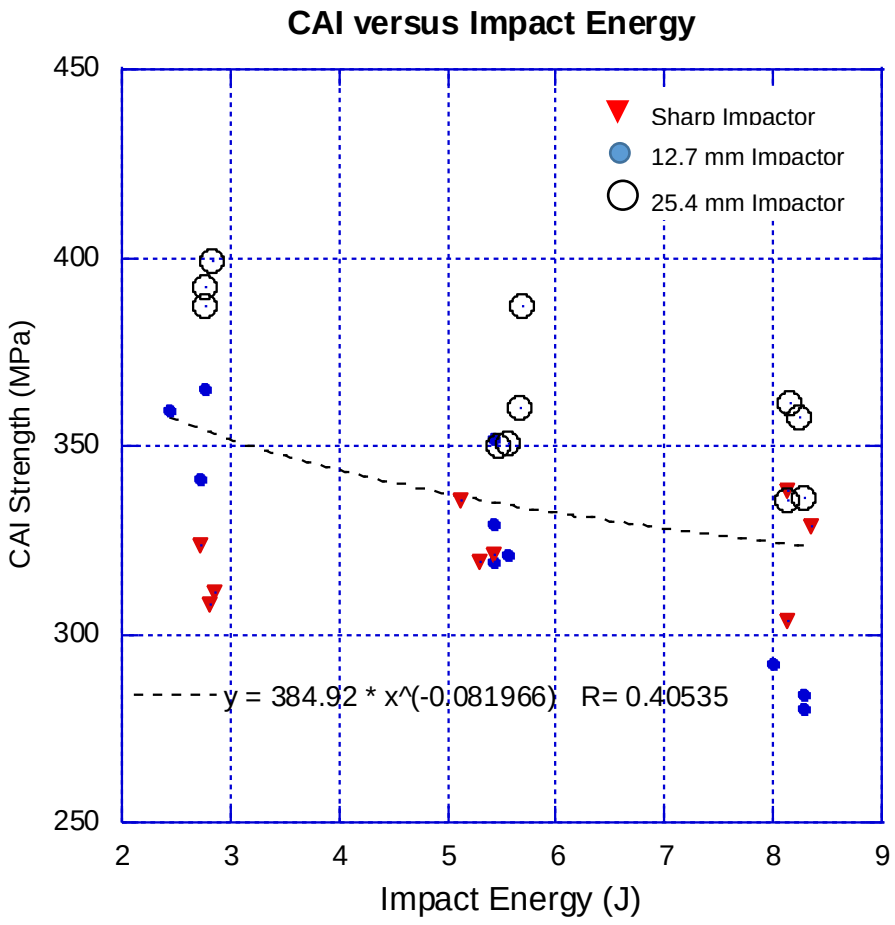

Figure 10. Graphic representation of CAI strength versus impact energy results obtained in this study.

It is apparent from figure 10 that at low impact energies, the sharp impactor will give a lower CAI strength result, but at higher impact energy levels, the CAI strength is higher for the sharp impactor than for the 12.7 mm impactor. The 24.5 mm impactor shows higher residual strengths at any given impact energy than the other two types of impactors tested. The middle impact energy shows little difference in CAI strength values. It appears that this is due to the sharp impactor giving a similar CAI strength value for all impact energy levels tested in this study, but the blunt impactors show the more typical (and expected) result of lower CAI strength values with increasing impact energy levels. At the highest impact energy used, penetration of the face sheet occurred for the sharp and the 12.7 mm impactors. The correlation coefficient of R=0.41 is a poor fit compared to data used from a single type of impactor [14].

Since in actual practice the kinetic energy of an impact event is not known, figure 11 shows CAI strength plotted versus damage width (a measurable post impact parameter). A “best fit” power curve was calculated and is plotted in the figure.

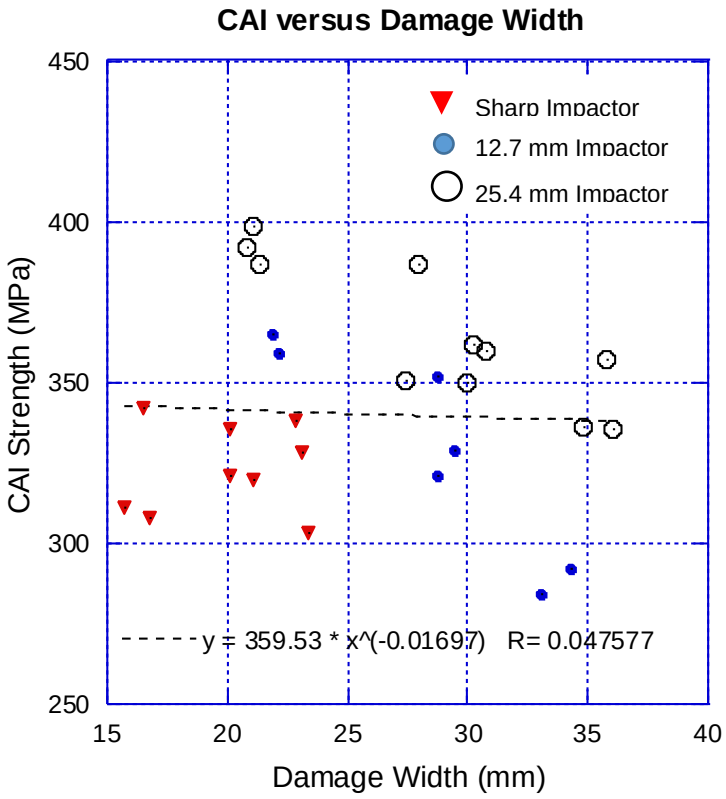

Figure 11. Graphic representation of CAI strength versus damage size results obtained in this study.

It is apparent that the claim in reference [14] that damage width as detected by thermography is a good indicator of CAI strength may not be true for different impactor shapes and sizes since at all damage sizes the CAI strengths of the sharp impactor are about the same and at the larger damage sizes, a larger blunt tipped impactor gives a higher CAI strength than a smaller blunt impactor. The correlation coefficient of R= .048 is quite poor.

Since damage dent depth (as measured by a dial gage) appeared to be “well behaved” (see figure 6) it may be of interest to examine a plot of CAI strength versus dent depth, which is also a measurable parameter after an impact event. The results are shown in figure 12 and seem to better represent the data for the sharp impactor and the power curve fit gives a correlation coefficient of R=0.68, which is the best fit thus far, although not as good as a fit as was found for one type of impactor in a previous study [14].

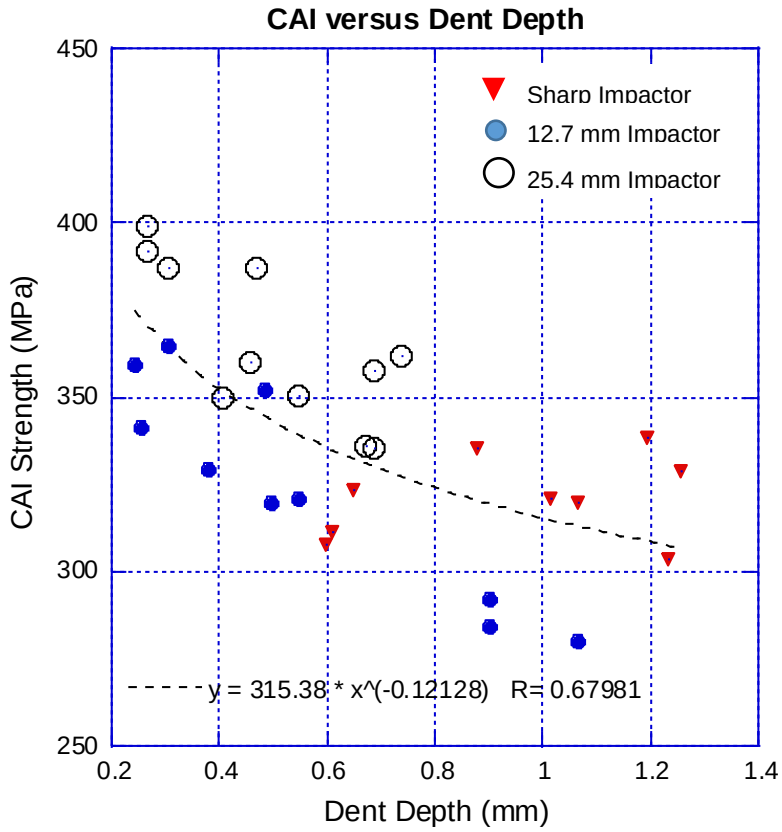

Figure 12. Graphic representation of CAI strength versus dent depth results obtained in this study.

Since it is apparent that both damage size and dent depth contribute to the CAI strength of the sandwich structure tested in this study, a plot of CAI strength versus damage size multiplied by dent depth (thus taking both parameters into account) is plotted in figure 13.

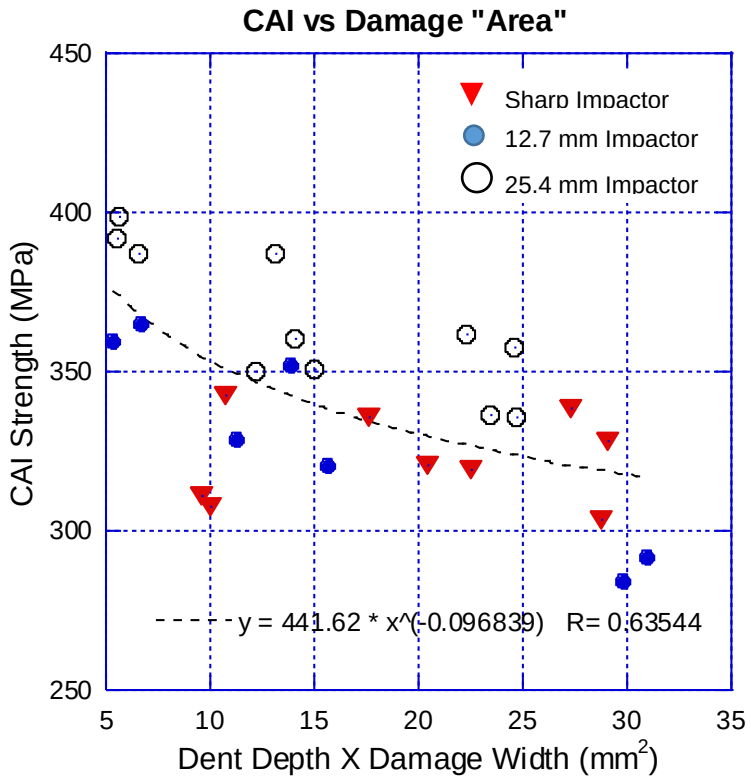

Figure 13. Graphic representation of CAI strength versus dent depth times area results obtained in this study.

The correlation coefficient of R= 0.64 is not quite as good as the power curve fit to the dent depth data. These results show that developing a CAI allowable for a variety of impacts that may occur to a piece of hardware, can be difficult to perform with any degree of fidelity, especially if a sharp object impacts the sandwich structure. Thus, it is suggested that a lower bound strain allowable (typically 4000 με) be used to cover all damage events as noted in [15]. It should be obvious when a part is so badly damaged that the 4000 με limit may not be low enough and thus a repair would be called for. Since the face sheet modulus is 60 GPa, this corresponds to a stress of about 240 MPa which is well below the lowest CAI strength values obtained in this study.

5.0 CONCLUSIONS

The effects of 25.4 mm and 12.7 mm diameter hemispherical impactors and a sharp impactor on the impact response (visual damage, dent depth and damage size as detected by thermography) and CAI strength of honeycomb core sandwich structure with carbon/epoxy face sheets has been investigated in this study. The results show that the impact response and resulting CAI strength values, especially of the sharp impactor, are different for the three types of impactors.

The visual damage is much easier to see with the sharp impactor which would be beneficial in actual practice since this increases the chances of an impact event being discovered.

For the two sizes of hemispherical impactors, the visual damage is similar until higher impact energies when the smaller hemispherical impactor begins to penetrate the face sheet.

The dent depth measurements were larger for the sharp impactor across all energy levels tested. The differences in dent depth of the two hemispherical impactors did not vary much until the highest impact energy level used (8.1 J) was reached where the larger impactor gave a smaller dent depth. This was due to the beginning of penetration of the face sheet for the 12.7 mm impactor at the 8.1 J energy level.

Thermography results showed the sharp impactor yielding a smaller damage zone for a given impact energy for all three impact energy levels tested. The difference in damage size between the two hemispherical impactors was not notably different.

The CAI results showed that the sharp impactor gave essentially the same CAI strength values regardless of impact energy or damage size. This suggests that at the three impact energy levels used in this study that the sharp tipped impactor essentially punctured a hole in the specimen and the specimen behaved as such giving a constant CAI strength value as if a hole of a given size was drilled through the face sheet. The CAI strength results for the hemispherical impactors was more "well behaved" in terms of showing a decrease in CAI strength with an increase in impact energy or damage size. Differences in CAI strength between the 12.7 mm and 25.4 mm impactors was most notably evident at the higher impact severity levels where the 25.4 mm impactor gave higher CAI strength values.

These results raise practical questions about using impact energy alone, or even measurable post impact parameters, as metrics to define an impact event, as is commonly done in "damage threat assessments" since the impact response and subsequent CAI strength can be quite different depending on the shape and size of the impactor. It is suggested to use a lower bound strain allowable rather than attempting to develop a CAI strength allowable based on testing using the typical methodology of using one hemispherical size impactor since in practice, any shape impactor may hit the piece of hardware.

REFERENCES

1. ASTM D 7136/D7136M-12. *Standard test method for measuring the damage resistance of a fiber-reinforced polymer matrix composite to a drop-weight impact event.* West Conshohocken, PA: ASTM International, 2012.
2. DeFrancisci GK, Chen ZM and Kim H. Low-velocity, high mass, wide-area blunt impact on composite panels, *Transportation Research Record: Journal of the Transportation Research Board* (2011); 2206: 1-9.
3. Poe CC. Impact Damage and Residual Tension Strength of a Thick Graphite/Epoxy Rocket Motor Case, *Journal of Spacecraft and Rockets* 1992; 29: 394-404
4. Nettles AT and Clark AM. *A damage resistance comparison of wet-wound IMT and T1100 carbon fiber/epoxy cylinders*, NASA Technical Memorandum 20220005181, April 2022.
5. Dalton, TK. *Advanced booster EDDR Final Report, Volume 6: Composite Case Reliability Assurance System (CCRAS) overall project summary,* Orbital ATK Report TR033091-06, April 2015.

6. Tomblin JS, Raju KS, Liew J and Smith BL. *Impact damage characterization and damage tolerance of composite sandwich airframe structures*, DOT/FAA/AR-00/44, January 2001.
7. Mitrevski T, Marshall IH, Thomson, R. The influence of impactor shape on the damage to composite laminates, *Composite Structures* 2006; 76: 116-122.
8. Elaldi F, Baykan B and Akto C. Experimental analysis for the effect of impactor geometry on carbon reinforced composite materials, *Polymers and Polymer Composites* 2017; 25: 677-682.
9. Cao, H et.al. Experimental investigation of impact diameter effect on low-velocity impact response of CFRP laminates in a drop-weight impact event, *Materials* 2020;13, 4131
10. Icten BM, Kiral, BG and Deniz ME. Impactor diameter effect on low velocity impact response of woven glass epoxy plates, *Composites: Part B* 2013; 50: 325-332.
11. Sevkat E, Liaw B and Delale F, Drop-weight response of hybrid composites impacted by impactors of various geometries, *Materials and Design* 2013; 52: 67-77.
12. Delaney MP, Fung SYK and Kim H. Dent depth visibility versus delamination damage for impact of composite panels by tips of varying radius, *Journal of Composite Materials* 2018; 52: 2691-2705.
13. Nettles AT, Barnes, BW, Guin, WE and Mavo. JP. The effects of impactor shape on the compression after impact strength of carbon/epoxy face sheet foam core sandwich structure, *Journal of Sandwich Structures and Materials* 2023; https://doi.org/10.1177/10996362231199099
14. Nettles AT and Jackson JJ. Compression after impact testing of sandwich composites for usage on expendable launch vehicles, *Journal of Composite Materials* 2010, 44: 707-738.
15. Nettles AT, Guin, WE and Mavo, JP. The effects of edge quality on the measured compression strength of quasi-isotropic composite specimens and its practical implication to the development of allowables, *Journal of Composite Materials* 2021, 5